J. Phys. A: Math. Gen. 27 (1994) 6741–6758. Printed in the UK

Hierarchical structure in the chaotic scattering off a magnetic dipole

B Rückerl and C Jung
Fachbereich Physik, Universität Bremen, 28359 Bremen, Germany

Received 6 July 1994

Abstract. We use the scattering off a magnetic dipole as an example of how a useful hierachical order can be found in the set of singularities of an appropriate scattering function. This function is an unusual type of time delay function. Knowledge of the hierachical order can be used to construct a symbolic description of the dynamics. Here it is useful to have a number of symbol values which are larger than the number of basic periodic orbits of period one.

1. Introduction

The best way to give a complete overview of the global behaviour of a chaotic system is to construct a symbolic dynamics. This will contain, in a very compact way, the qualitative structure of the set of all trajectories. (For some general ideas on symbolic dynamics and some applications of them on open systems see [1–7].) Unfortunately, for most systems there is no chance to construct an exact symbolic dynamics with a finite number of grammatical rules. However, it is helpful to have at least some approximate symbolic description which properly captures the dynamics over time intervals in some finite range. The purpose of this paper is to present some steps towards this goal for the case of chaotic scattering systems. We demonstrate our ideas with the aid of the scattering of an electrically charged particle off a magnetic dipole, the so-called Störmer problem [8]. It has been shown numerically that this system contains topological chaos in its bound trajectories [9–11] as well as in its scattering behaviour [12]. For this system, there is even analytical proof that it is not completely integrable [13]. The practical interest in this model lies in the description of the motion of charged cosmic particles in the magnetic field of the earth.

In the case of chaotic scattering (for reviews see [14, 15]), scattering functions, for example the time delay function or the deflection function, contain singularities on a fractal subset of their domain. This behaviour has the following explanation. For positive ranges of the energy there also exists a chaotic invariant set (the so-called chaotic saddle) containing an infinite number of unstable localized orbits whose invariant manifolds reach out into the asymptotic region. Whenever a scattering trajectory starts close to the stable manifold of the saddle, it approaches the localized orbits, runs for a while alongside them and, for a finite time, traces out complicated motion of the type which chaotic localized orbits perform for ever. Thereby, scattering chaos is a version of transient chaos. When the scattering trajectory starts exactly on a stable manifold of the saddle, it stays in the saddle for ever and is captured. Of course, this can happen only for a subset of measure zero in the set of all possible initial scattering asymptotes. For such particular initial conditions, the delay time is infinite and the deflection angle is undefined. Therefore, the singularity structure of the scattering function presents the fractal structure of the bundle of stable manifolds of the

0305-4470/94/206741+18$19.50

chaotic saddle and, therefore, provides many characteristic numbers of the chaotic saddle itself [16]. The appropriate method to obtain such numbers (e.g. entropies, dimensions, Lyapunov exponent, escape rate) numerically is the thermodynamic formalism [17, 18].

Scattering chaos of this type has been found in a large variety of systems, e.g. in classical models for molecular reactions (for these processes see the review [19]), in model computations for satellite encounters [20], for vortex scattering in hydrodynamics [21], in soliton scattering [22], for particle transport in an open hydrodynamical flow [23] and for various models of potential scattering. For a recent overview of this field of activity see the feature issue of the journal *Chaos* on chaotic scattering [24].

The first step in the analysis of a chaotic scattering system should consist of finding some systematic order in the singularity structure of the scattering functions. In particular, a hierarchical order is needed. The main purpose of this paper is to show, with the aid of the particular example of scattering off a magnetic dipole, how such an order is obtained in a natural way. For comparison, we present three different scattering functions for this model and, in section 4, we demonstrate how one of them, namely, a particular variant of the time delay function, orders its singularity structure in a very useful hierarchical way. We shall make essential use of some ideas already presented in [7]. Therefore, let us give a very short review of the main considerations of this paper: the basic structure of the invariant set is represented as a horseshoe construction in an appropriate Poincaré map [25]. In particular, its skeleton is given by the homoclinic grid of some fixed point. If the system has a local potential with a barrier which acts as an outer boundary for the invariant set, then the most appropriate fixed point is the one belonging to the unstable periodic orbit oscillating over the barrier. Under variation of some system parameters, the tendrils of the invariant manifolds and, therefore, the homoclinic grid also change and, in particular, they create homoclinic bifurcations whenever some tendrils of the stable and unstable manifolds touch each other tangentially. Then, the horseshoe construction is not completely hyperbolic and in the invariant set there are also KAM tori at least on a small scale. This prevents the construction of a finite exact grammar for a symbolic description. However, in between the parameter space, there are also intervals in which homoclinic bifurcations are avoided (at least on low levels of the hierarchy), even though the invariant set is not a complete horseshoe. In such intervals, a hierarchical order of the homoclinic grid can be described with a finite number of rules (at least approximately). This order also applies to the structure of the scattering functions. For some more information on the possibility of finite and exact grammatical rules and hyperbolicity for incomplete horseshoes see also [26, 27].

2. Singularity structure in the scattering functions

Imagine a magnetic dipole of moment μ oriented along the z-axis and sitting in the origin of position space with coordinates $q = (x, y, z)$. The vector potential of its magnetic field is given by

$$A(q) = \mu(y/r^3, -x/r^3, 0). \tag{1}$$

Here, r is the absolute value of q. The Hamiltonian of a particle with electric charge Q moving in this field is given by

$$H = (p - QA(q)/c)^2/2m \tag{2}$$

where p is the momentum of the particle, m is its mass and c is the speed of light. Because of the rotational symmetry of the system about the z-axis, the z component of the angular momentum is conserved and we can separate off one degree of freedom. We transform to the cylindrical coordinates ρ, ϕ, z, forget about the ϕ coordinate, scale out all parameters as shown in [11] and obtain the motion of a particle in the following two-dimensional local potential

$$V(\rho, z) = (1/\rho - \rho/r^3)^2/2. \tag{3}$$

For some contour lines of this potential see [12]. The only parameter left in the system is the total energy E and, in the following, we will investigate how the invariant set changes under variation of E. There is a bifurcation energy $E_s = 0.081\ldots$ above which the system has no localized orbits. Accordingly, for $E > E_s$ all scattering functions are smooth. At E_s a chaotic saddle is created. The central bifurcation at E_s is a saddle-centred bifurcation between a hyperbolic orbit γ and an elliptic orbit Γ, both of which cross the plane $z = 0$ once from above and once from below during each revolution. Accordingly, we will call these period-one orbits. At some lower energy, the orbit Γ becomes inverse hyperbolic. These two orbits are the backbone of the chaotic saddle. For $E > E_{1-} = 0.0605\ldots$ no further orbits of period one exist. Figure 1 shows the two periodic orbits γ and Γ and a typical scattering orbit in the ρ–z plane for $E = 0.074$. Some more trajectories for other energies are plotted in [12]. The potential (3) has a barrier of height $E_b = 1/32$ such that for $E < E_b$, the chaotic set lies behind the barrier, is no longer accessible to scattering trajectories and the scattering functions become smooth again, i.e. scattering chaos only exists in the energy interval $I_c = (E_b, E_s)$.

The structure of the chaotic set in the scattering function depends strongly on the value of E. In complete analogy to the system investigated in [7], there exist parameter intervals

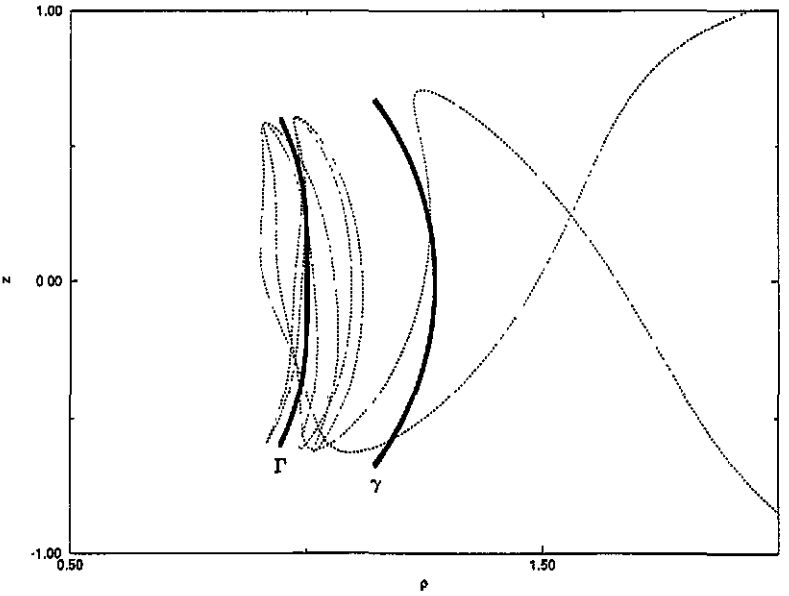

Figure 1. A plot of the two orbits of period one shown as full curves and a typical scattering trajectory as a broken curve in the ρ–z plane. γ is the outer and Γ the inner periodic orbit. The value of the energy is $E = 0.074$.

I_α in which the structure of the invariant set can be described rather well by finite rules and complements in which a symbolic description is extremely complicated. The intervals I_α are the ones in which homoclinic tangencies are avoided, at least in low levels of the hierarchy. For more explanations see below and [7].

There exists an energy interval $[E_{1-}, E_{1+}] = [0.0605, 0.0645]$, which we call I_1, in which a completely hyperbolic binary chaotic saddle is realized in a Poincaré map of the system. Then, a binary symbolic dynamics with trivial grammatical rules applies, i.e. all symbol sequences in two-symbol values are realized. To demonstrate our ideas on the construction of a useful symbolic description, let us choose an energy value for which the rules are not so trivial. We choose $E = 0.074$, which lies in the parameter interval $I_{1/2}$ in the terminology of [7]. $\alpha = \frac{1}{2}$ means that the binary horseshoe construction has already been disentangled halfway.

This can be explained better in an appropriate Poincaré section. There are two different quite natural choices for a Poincaré plane which are both adapted to the symmetry $z \to -z$ and $p_z \to -p_z$ of the system, namely the plane $z = 0$ and the plane $p_z = 0$. In both of these planes, we use both orientations of intersection of the plane in order to reduce out the symmetry and we monitor at each intersection the values of ρ and the corresponding momentum p_ρ. Then, the periodic orbit γ corresponds to a fixed point x_0 of the Poincaré map in the ρ–p_ρ plane. Figure 2(a) shows the homoclinic tangle created by the invariant manifolds of x_0 in the plane $p_z = 0$ and figure 2(b) is the corresponding picture in the plane $z = 0$. Some tendrils of the stable manifold W^s and of the unstable manifold W^u are plotted. These two choices of intersection plane have the following advantages and disadvantages. In the plane $p_z = 0$, the fundamental curvilinear rectangle of the horseshoe construction (it is drawn as a full curve in the plot and its corners are labelled by x_0, y_2, y_1, y_3) lies symmetrically with respect to the ρ-axis and its hierarchical construction scheme can be grasped easily. In contrast, in the plane $z = 0$, the fundamental rectangle is distorted asymmetrically and the tendril hierarchy level is also shifted. Therefore, we will use the plane $p_z = 0$ for high energies. As we will explain later, for lower energies the Poincaré section in the plane $p_z = 0$ becomes discontinuous. Therefore, for such lower energies it is advisable to use the plane $z = 0$ in spite of its small disadvantages. The tendrils in figure 2 are approximately half the length they would need to be to build a complete horseshoe construction. Therefore, we call this the case for which the disentanglement parameter α has the value $\frac{1}{2}$. For a more precise definition of parameter α see [7]. Compare figure 2(a) of the present paper with figure 2 in [7].

The tip of tendril number n of W_s or W_u is labelled by t_{sn} or t_{un}, respectively, in the figures. Points labelled by the same letters in parts (a) and (b) are related as follows. Take a point p in the plane $z = 0$ shown in figure 2(b). Follow the trajectory in phase space through this point until it intersects the plane $p_z = 0$. This point of intersection is also labelled by p. The composition of this canonical map from the plane $z = 0$ into the plane $p_z = 0$ with the corresponding map from the plane $p_z = 0$ into the plane $z = 0$ forms just the original symmetry-reduced Poincaré map in the plane $z = 0$. By this transfer of structures between the two planes, the hierarchical levels of the structures in the plane $z = 0$ are the levels taken from the plane $p_z = 0$ and transported into the other plane. Correspondingly, the hierarchical ordering in the plane $z = 0$ is not symmetrical with respect to the line $p_\rho = 0$ in this plane. It is also possible to introduce a symmetrical order of levels in the plane $z = 0$. However, then we can no longer use a fundamental rectangle to perform the horseshoe construction. Instead, we must use the area between the local segments of W_u and W_s, which are the direct connections between the points x_0 and y_2, as a fundamental

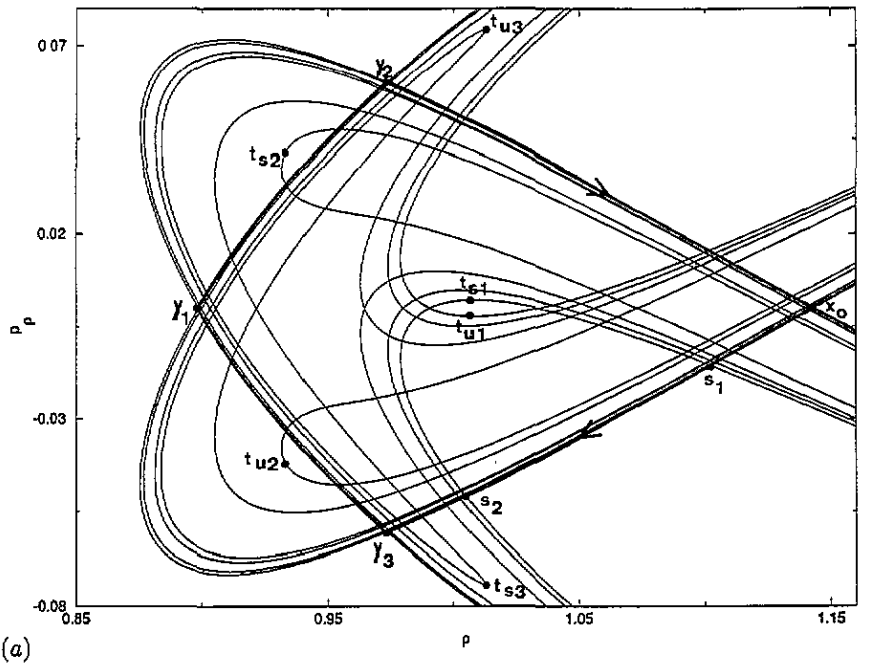

(*a*)

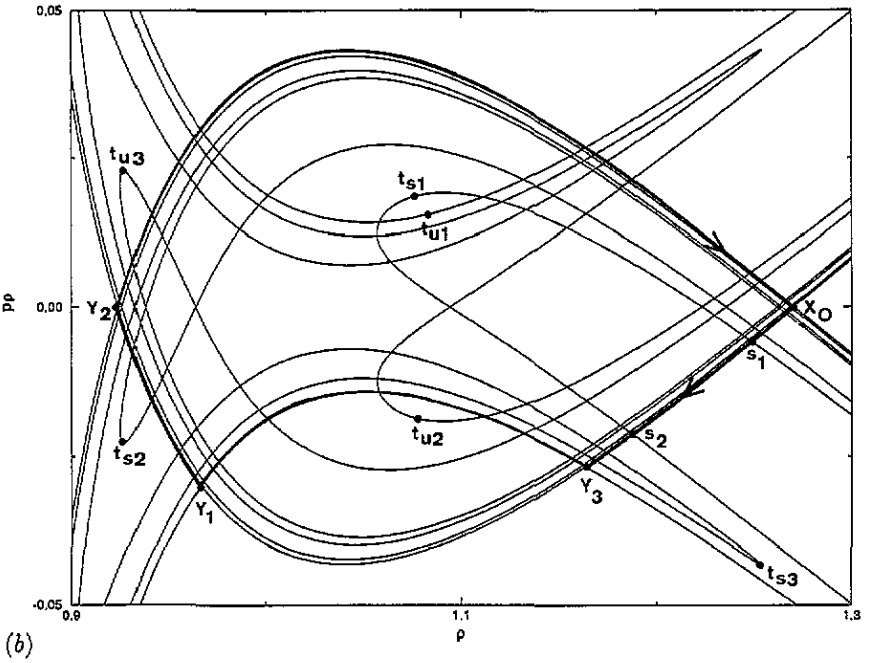

(*b*)

Figure 2. In a Poincaré section defined by the intersection condition $p_z = 0$ in (*a*) and $z = 0$ in (*b*), we use the coordinates ρ and p_ρ. x_0 is the fixed point of the Poincaré map corresponding to the periodic orbit γ. Pieces of the invariant manifolds of x_0 are also shown. Tendrils up to level 4 are plotted. The tips of the tendrils of level n are labelled as t_{sn} and t_{un} for W_s and W_u, respectively. The fundamental rectangle of the horseshoe construction (i.e. the rectangle with corners x_0, y_2, y_1, y_3) is given by the full curves. The energy is $E = 0.074$.

area. Of course, this area is also a completely satisfactory covering of the chaotic saddle of the map. For an example of this construction, see section 5.

Figures 3 and 4 present the time delay function and the deflection function for energy $E = 0.074$. They have been obtained as follows. We fix some value ρ_{in} sufficiently large such that it lies well inside the asymptotic region. Further, we fix $p_z = 0$, set $p_\rho = -(2E)^{1/2}$ and scan z_{in}. We follow each scattering trajectory until it reaches the outgoing asymptotic region again at some value ρ_{out}. The total time $T(z_{in})$ needed by the trajectory is monitored as a function of the initial variable z_{in}. Since we are only interested in the time delay that the trajectory had in the interaction region and not in the time it needed to enter and leave up to the asymptotic initial and final points, we subtract the asymptotic times and compute the function

$$Dt(z_{in}) = T(z_{in}) - \rho_{out}/p_{\rho,out} + \rho_{in}/p_{\rho,in}\,. \tag{4}$$

This function is plotted in figure 3. In addition, we monitor the direction of the outgoing trajectory represented by its angle relative to the plane $z = 0$. This deflection angle is plotted in figure 4 as a function of z_{in}. We see identical singularity structures in these two functions. However, it is nearly impossible to see a clear hierarchical structure. Whereas it is rather hopeless to try to get some ordering scheme out of the deflection function, for the time delay there is the following recipe [16–18] to enforce some fractal hierarchy by cutting the z_{in}-axis into intervals: on level n choose the threshold $Dt = n$, find all intervals I_j^n such that $Dt > n$ inside and $Dt < n$ outside. In the limit $n \to \infty$, this provides a fractal structure in which the boundaries of the intervals I_j^n accumulate towards the singularities of the scattering functions. This hierarchical construction of a Cantor set along the z_{in}-axis provides all the important characteristic numbers of the saddle, at least as long as it is hyperbolic. An inspection of figure 3 shows that this method does not provide any obvious and simple scheme. On the other hand, figure 2 shows that the homoclinic intersection grid is rather regular and this regularity implies the same type of simplicity in the whole saddle and should be transfered into the scattering behaviour. The structure of the bundle of stable manifolds going out into the incoming asymptotic region is exactly the structure given by the intersection of the stable manifolds with that short segment W^u_{loc} of the unstable manifold of x_0 which starts directly from the point x_0 (it is the full curve between the points x_0 and y_3 in figure 2(a)). Figure 2 indicates that we have a situation where all the tips of the tendrils of W^u are located in gaps void of tendrils of W^s and *vice versa*. Then, under iteration of the map, each tip is mapped out of the area containing homoclinic intersections after a finite number of iterations (compare similar considerations in [26]). Therefore, there should be appropriate scattering functions which reveal this structure and provide a good starting point to construct a symbolic description of the structure. In the next section, we show an example of such a function.

3. Modified delay function

We saw that the time delay function can be used to construct some hierarchical fractal structure. However, the result is not yet satisfactory. So, we try to improve it and construct a better-suited function which we shall call the modified delay function. The motivation for its construction is provided by the following reasoning. The starting point for any horseshoe construction in a map, such as, for example, the Poincaré map of the given scattering system, is a fundamental area A which is stretched and folded in any application of the map, such

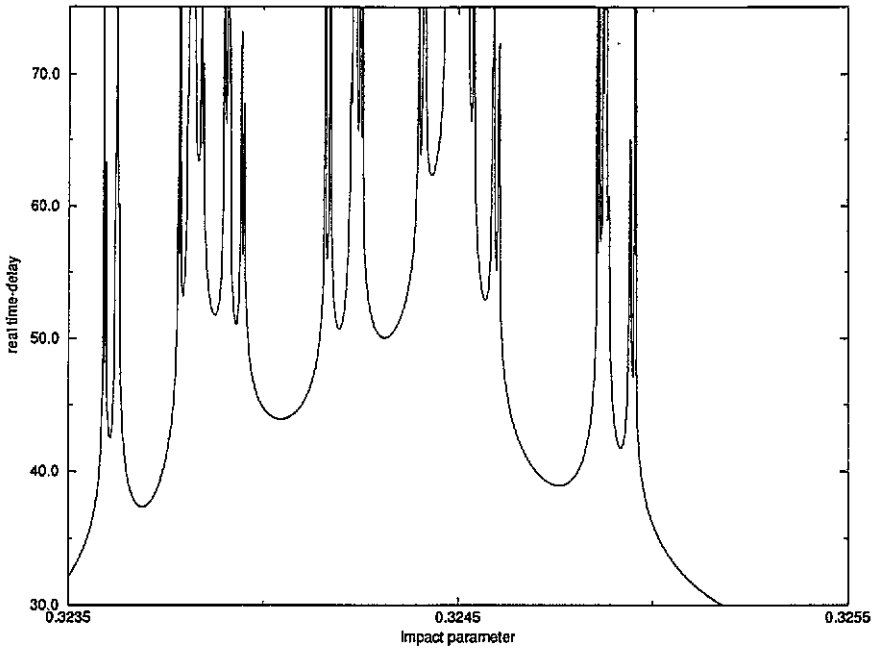

Figure 3. Time delay function for $E = 0.074$ as a function of z_{in} for fixed incoming momentum in the negative ρ-direction.

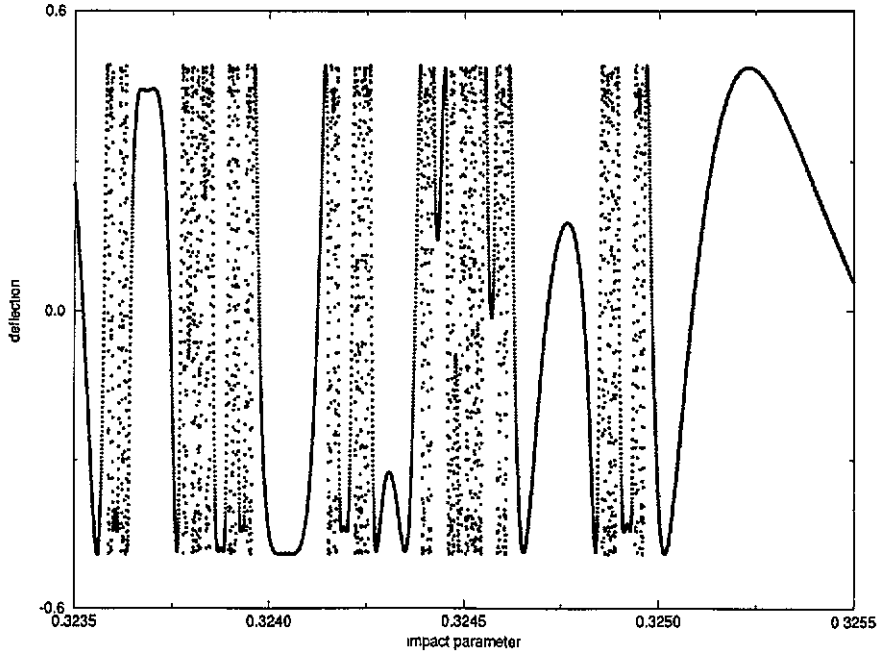

Figure 4. Deflection function for $E = 0.074$. The outgoing angle is plotted against z_{in} for fixed incoming direction, as in figure 3.

that A covers all points which are not mapped to infinity under iterated application of the map. The hierarchical structure of the horseshoe is obtained by iteratively cutting out subregions of A containing points not leaving A after n iterations. Thereby any generic trajectory of the phase space (domain of the map) not belonging to the chaotic saddle itself can be assigned, as a label, the number of its iterates lying inside the fundamental area A. We apply this idea of labelling scattering trajectories to our system. First, we choose an appropriate plane for a Poincaré map. In our case, it is the plane already introduced above, i.e. the intersection condition is $p_z = 0$. The homoclinic grid of figure 2(a) shows us what a good choice for the fundamental area the region A enclosed by the full curves is. It is the curvilinear rectangle with the corners x_0, y_2, y_1 and y_3 where the boundaries are formed by segments of the invariant manifolds of the fixed point x_0.

The potential equation (3) has a saddle point at $\rho = 2$, $z = 0$ and for larger values of ρ outside of the saddle it decreases monotonically; there are no localized orbits beyond the saddle point. Trajectories crossing this potential saddle from the inside to the outside will never return. The orbit γ oscillating on this saddle of the potential divides the position space into an inside and an outside region. Complicated motion only occurs in the inside region. In phase space, the invariant manifolds of γ divide regions of complicated behaviour from regions of simple behaviour. The manifolds of x_0 in the Poincaré plane enclose the region containing periodic points and localized trajectories.

Now, the prescription for the modified delay function is as follows. Take some one-dimensional line in the set of initial asymptotes, e.g. fix the values of E and p_z and choose a large value of ρ which is well into the asymptotic region and scan the initial value of z. Run scattering trajectories, watch for their intersections with the Poincaré plane and count the number M of intersections inside A as a function of some curve parameter s of the line of initial asymptotes. The resulting function $M(s)$ is the modified delay function. Figure 5 shows $M(z_{\text{in}})$ for the magnetic dipole where all parameters as well as its domain are the same as they are for the other two scattering functions shown in figures 3 and 4. Figure 6 gives a magnification of figure 5 in order to show the regular structure contained

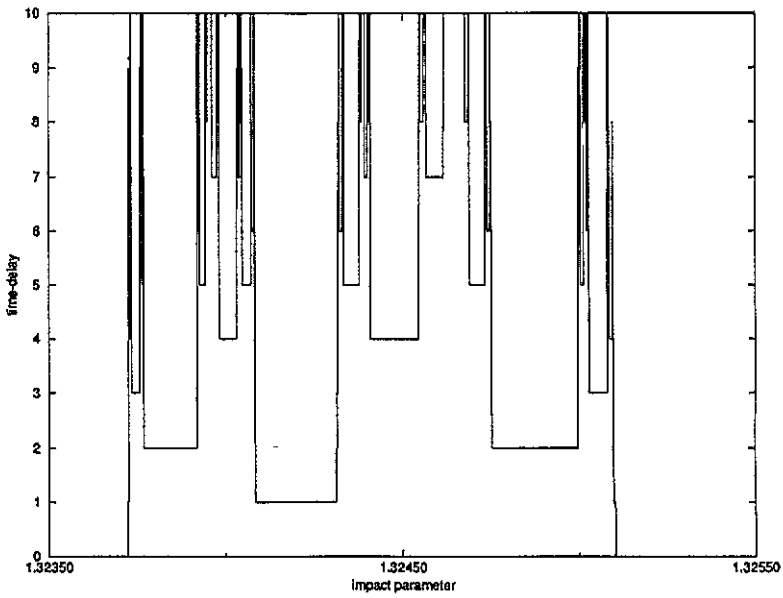

Figure 5. Modified delay function for the same parameters as those used for figures 3 and 4.

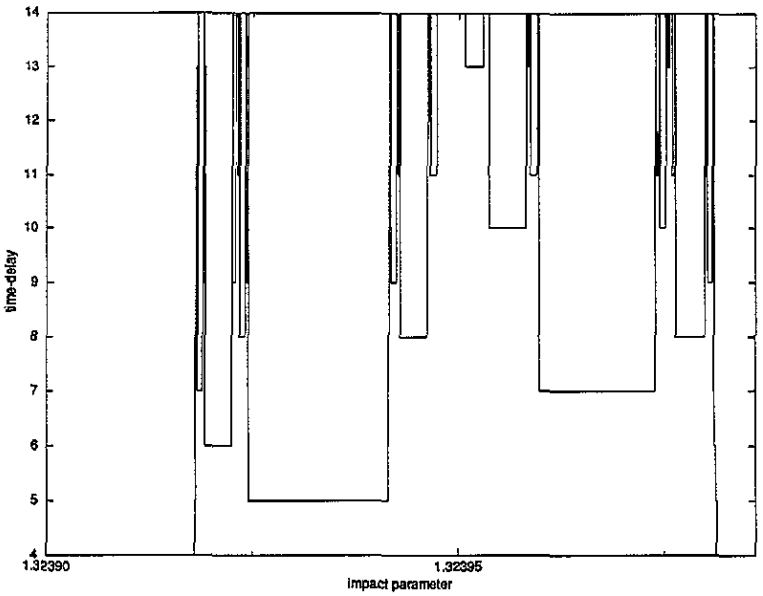

Figure 6. Magnification of a part of figure 5.

in this function. Of course, the discontinuities of this new function exactly coincide with the discontinuities of the other two scattering functions.

The values of the function M are integers and, therefore, provide a natural hierarchical Cantor-set construction along the z_{in}-axis by cutting out in step n such intervals in which $M \leqslant n$. In step n, the intervals J_j^n in which $M > n$ remain.

Let $N(n)$ be the number of intervals J_j^n on level n. The ratio

$$B = \lim_{n\to\infty} N(n+1)/N(n) \tag{5}$$

is the branching ratio of the singularity structure and $K_0 = \ln(B)$ is its topological entropy.

4. Symbolics of the branching tree

The intervals J_j^n create a branching tree as follows. On level n, each interval J_j^n is represented by one entry. This is connected with the entry of the interval $J_k^{(n-1)}$ of level $n-1$ if $J_j^n \subset J_k^{(n-1)}$. The resulting tree is presented up to level 5 in figure 7.

This hierarchy of partly nested intervals coincides with the hierarchy we obtain from the homoclinic tangle. It is sufficient to consider the homoclinic intersections along the local segment W_{loc}^u of W_u; it is the arc connecting x_0 with y_3. All other homoclinic points are some iterates of these and identified by J_1^0. The first-level tendril of W^s (its tip is labelled by t_{s1} in figure 2) cuts out the interval (s_1, s_2) and leaves two smaller intervals J_1^1 (the segment of W_u from x_0 to s_1) and J_2^1 (the segment of W_u from s_2 to y_3). In the next step, take the second-level tendril of W^s which is the pre-image of the first-level tendril and which cuts out parts of the first-level intervals J_k^1. The remaining intervals are from level 2. By continuation of this procedure, we obtain a nested-interval construction which

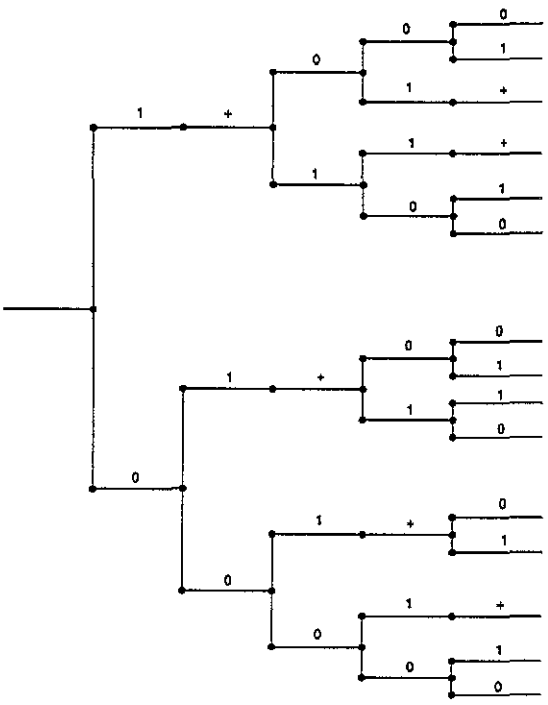

Figure 7. Branching tree for the disentanglement parameter value $\alpha = \frac{1}{2}$. Each entry is labelled by the last digit of its symbolic code in three symbol values.

is identical to the one created by the modified delay function and we also obtain exactly the same branching tree.

Next we need a symbolic dynamics describing this tree. The simplest and most natural dynamics we found is shown in figure 7, where the last digit of the label of each entry is given. The complete label of an entry of level n is a string of length n. It has the following very simple grammatical rules:

(i) on a string ending on 0, +1 or 1+, it is allowed to append either 0 or 1; and

(ii) on a string ending on 01 or on 11, it is only allowed to append +.

In order to obtain the lowest levels of the tree, we can imagine that the entry of level 0 has a 0 as its symbolic code. We see that whenever some interval is not cut into two pieces in a transition from one level to the next, the symbol + is appended in order to obtain the label of the new interval of the higher level. When an interval is cut into two pieces, the symbols 0 and 1 are appended to the label of the old interval in order to obtain the two labels of the new intervals. The rule for the distribution of the 0 and 1 is as follows. When the label of the old interval contains an even number of 1's, the right-hand new interval gets the 0 and the left-hand new interval the 1. When the label of the old interval contains an odd number of 1's, it is the other way around.

At first it may seem strange to use three different symbol values (namely 0, 1, +) for a horseshoe which contains only two points of period one and which is an incomplete version of a binary horseshoe and, of course, there are also possibilities to construct symbolic dynamics with an alphabet containing two symbols only. However, these possibilities have important disadvantages. Any effort to label the branching tree as it stands in figure 7 with two symbol values leads to infinite rules. In order to enforce a description with two symbol values and finite rules, it is necessary to split all such entries which are labelled by + in figure 7 into two parts and to treat these two parts as two disjoint intervals in the two-symbol description. This procedure is acceptable from the point of view of constructing

some partition of the Poincaré plane which generates the symbolic dynamics. In the case of the three-symbol description, the partition is made by segments of W_u and W_s only, but this is not true for the use of the two-symbol description. The artificial division is unnatural from the point of view of scattering processes, where the partitions should be given by the scattering-process continuity intervals and their scattering functions. Nevertheless, let us give here for comparison a possible symbolic description in two-symbol values. The branching tree is given in figure 8. Comparison with figure 7 shows that now all the entries having the last symbol + in figure 7 are split into two entries in figure 8. To make this evident, these entries are connected in figure 8 by a broken vertical line. The last digit of the labels in two-symbol values is indicated in the figure. The complete label of each entry of level n is again a string of length n. The labels in figure 8 obey the following grammatical rules:

(i) on a string ending on 000, 001, 100, 101 or 110, it is allowed to append either 0 or 1;

(ii) on a string ending on 010 or 011, it is only allowed to append 0.

The topological entropy coming from these rules is exactly the same as the one coming from the other rules in three-symbol values given above. Its numerical value is $K_0 = 1.7\ldots$. These rules are valid in the interval $I_{1/2} = [E_{1/2-}, E_{1/2+}] = [0.0711, 0.0744]$.

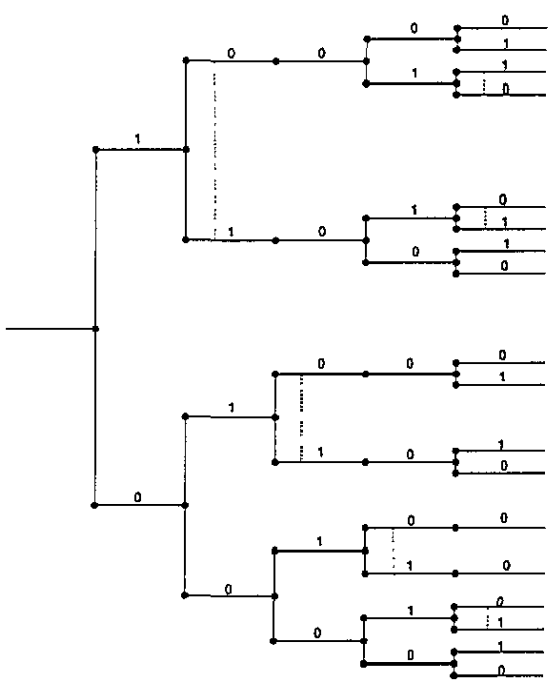

Figure 8. Branching tree for the disentanglement parameter value $\alpha = \frac{1}{2}$. Compared to the tree of figure 7 such entries, which have the last-symbol value + in figure 7, have been split artificially into two entries. Each entry is labelled by the last digit of its symbolic code in two-symbol values.

In these rules, the symbol string containing 0's only is allowed. It corresponds to the hyperbolic orbit γ and its occurrence shows that γ is accessible for scattering trajectories. The orbit Γ corresponds to the symbol string containing 1's only. This string is forbidden because for $E \in I_{1/2}$ the orbit γ is screened behind KAM lines and is not accessible to scattering trajectories.

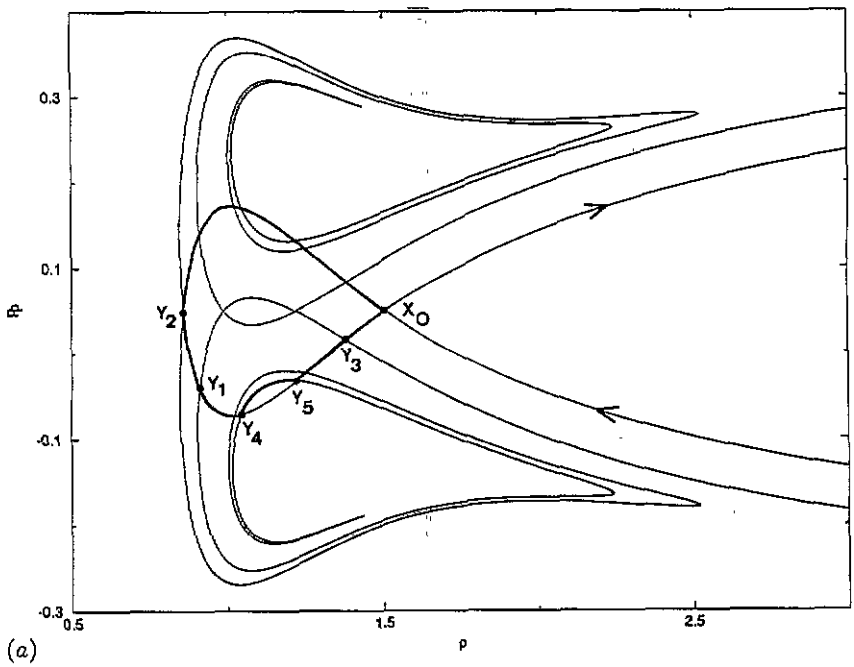

(*a*)

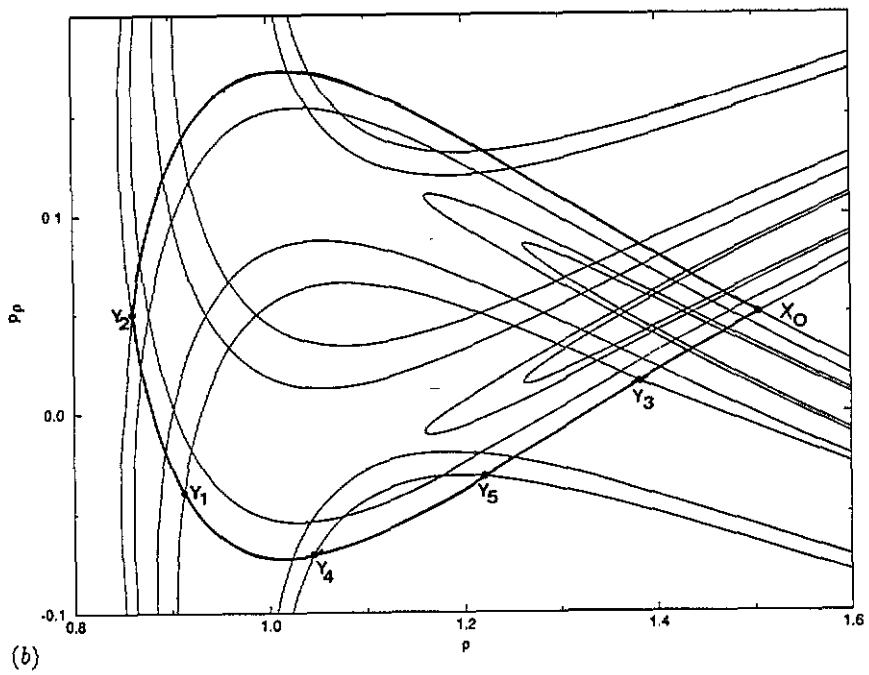

(*b*)

Figure 9. Homoclinic tangle of the fixed point x_0 in the Poincaré plane $z = 0$ for $E = 0.057$. Part (*a*) gives the tendrils up to level 1 in a rather large frame in order to demonstrate the way the tendril winds back. Part (*b*) shows tendrils up to level 2 in a smaller frame containing the fundamental rectangle. The fundamental rectangle (the one with the corners x_0, y_2, y_4, y_5) is marked by full curves.

5. Different parameter intervals

So far we have considered one particular value of the parameter E. In the energy interval $[E_{1+}, E_s]$, all the parameter intervals exist which have also been investigated and explained in [7]. Interestingly, in the magnetic dipole there exist cases not present in the system of [7]. In the present system, the parameter interval I_1, in which a binary horseshoe is complete, has a lower end at an energy $E_{1-} = 0.0605\ldots$ and for energies below this the horseshoe has more parts than in the complete binary case. This is caused by the following effect. Invariant-manifold tendril tips bend back towards the area A and pierce the other manifolds again. This is connected with the creation of further periodic points by saddle-centre bifurcations. See also figure 2 in [12].

In figure 9(a), we present the homoclinic tangle of the fixed point x_0 for the energy value $E = 0.057$, which is a good example of where the topological entropy is larger than ln(2). Here, the Poincaré plane is $z = 0$. In this large frame, we clearly see how the manifolds spiral back. Without these spiral effects, we would have a complete binary horseshoe construction. Figure 9(b) gives a magnification of the interior part showing in better resolution the homoclinic intersection points. All tendrils up to hierarchical level one are included in (a) and tendrils up to level 2 are included in (b). The fundamental rectangle of the horseshoe construction is again marked by full curves. Please note that it is not the continuation of the rectangle marked in figure 2. Now that the rectangle with the corners x_0, y_2, y_1, y_3 does not cover the complete area containing homoclinic intersection points, the winding back of the tendrils creates additional intersections outside. However, the rectangle with the corners x_0, y_2, y_4, y_5 (i.e. the one marked in the figure) does the covering. As explained above in the plane $z = 0$, we must make a choice which is not symmetric to the ρ-axis. An alternative satisfactory choice for A, which is symmetric but not a curvilinear

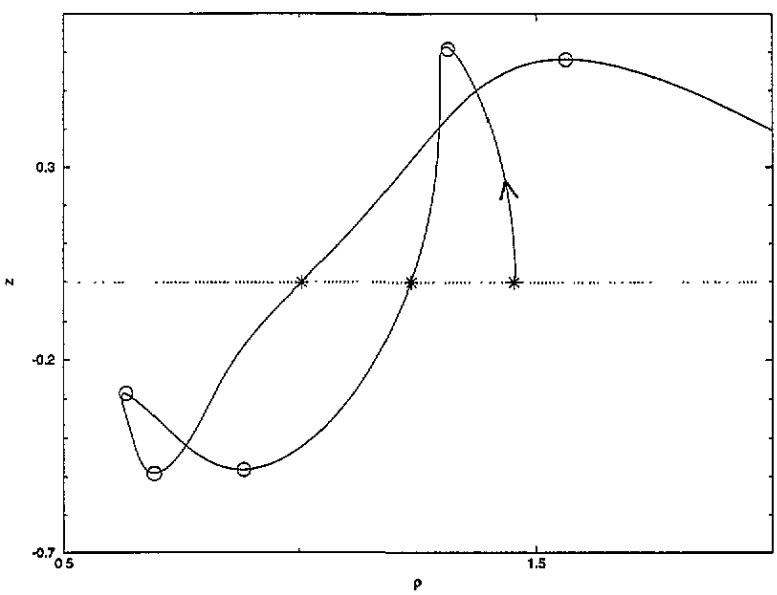

Figure 10. A segment of a trajectory belonging to W^u of x_0 plotted in the ρ–z plane. Intersections with the plane $z = 0$ are marked by crosses. Intersections with the plane $p_z = 0$ are marked by circles. Note that the crosses and circles do not follow each other alternatively.

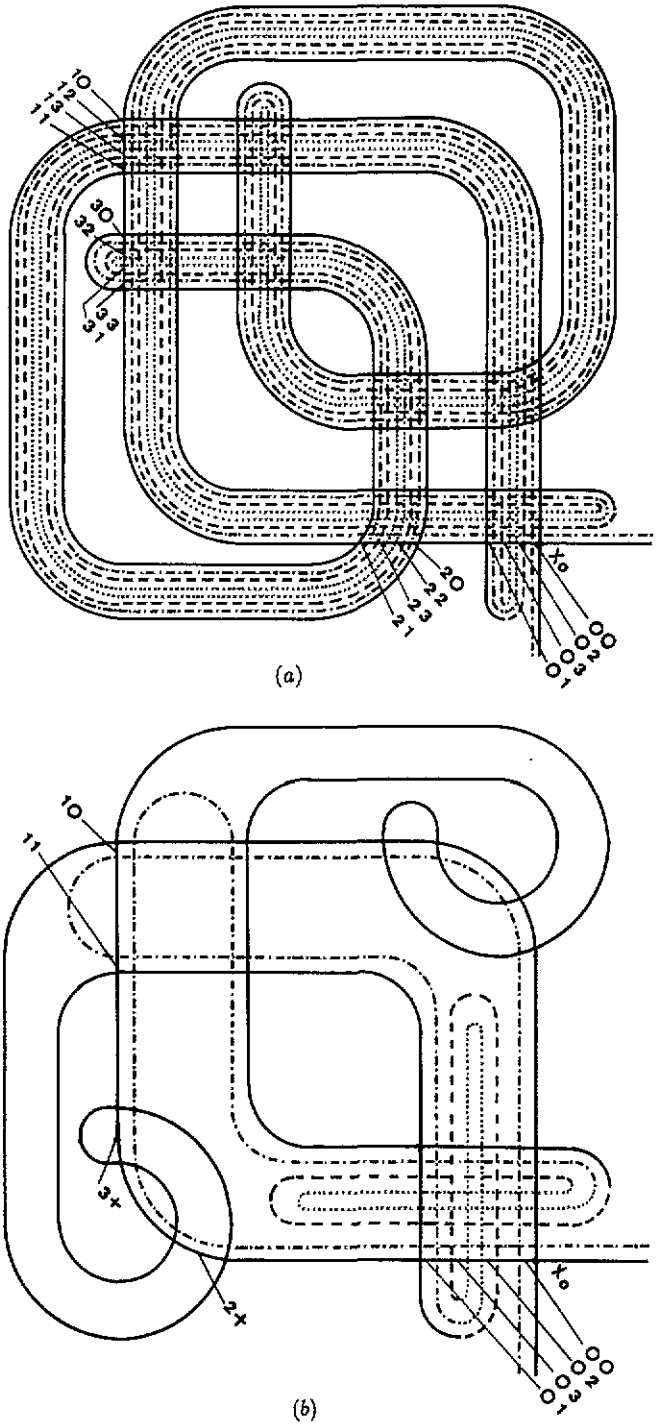

Figure 11. Part (*a*) gives the schematic plot of a complete horseshoe with four fixed points. Part (*b*) gives the schematic plot of the particular incomplete horseshoe which corresponds to the numerically constructed homoclinic grid of figure 9. Tendrils up to level 2 (in a symmetrical ordering scheme) are plotted. For better distinction, various segments are plotted in different line styles. Note that the structure in (*b*) is topologically the same as in figure 9.

rectangle, is the area enclosed by the local segments of W_u and W_s which connect x_0 with y_2 directly.

Now let us explain why we need the plane $z = 0$ for $E < E_{1-}$ and why we can no longer use the plane $p_z = 0$ in the same way as before. Figure 10 shows a segment of a trajectory belonging to W^u of x_0 in the ρ–z plane. Its intersections with the plane $z = 0$ are marked by crosses and its intersections with the plane $p_z = 0$ are marked by circles. Strikingly, between the second and third cross there are three different circles. This means that the Poincaré map in the plane $p_z = 0$ has discontinuity lines along which the continuation of an image line is provided by the third application of the map. We want to avoid this type of complication, which occurs in the plane $p_z = 0$, as soon as $E < E_{-1}$ and, therefore, use the plane $z = 0$.

The structure presented in figure 9 is an incomplete horseshoe of four fixed points. In the schematic figure 11(a), we show a corresponding complete horseshoe of four fixed points and in figure 11(b), we show the schematic situation corresponding to the numerically constructed figure 9 for the dipole. In the schematic figure 11, tendrils up to level 2 are included. For easier comparison between (a) and (b), various segments of the manifolds are plotted by different line styles such that equal line styles belong to corresponding segments. Full curves are the segments up to level 1. The level-2 segments are plotted as various broken curves. Along the local piece of W^u, the intervals cut out by the tendrils of W^s are labelled by the symbols 0, 1, 2, 3, +. Note that, compared to the complete situation, in the incomplete case of part (b) some intervals belonging to the symbol values 0 and 1 on the second level are fused into a single interval. To such an interval we will assign the symbol +, in complete analogy to the case of the interval $I_{1/2}$ shown above. For this parameter value, we do not have to deal with intervals resulting from the fusion of other combinations of basic symbol values. Therefore, it is sufficient to introduce the single additional symbol +. For other parameter values it might be appropriate to introduce further additional symbols denoting the fusion of other combinations of basic symbols.

The symbolic code for the parameter case $E = 0.057$ is again found most easily in the branching tree, which is given in figure 12 up to level 4. Each entry is labelled by the last digit of its symbolic code. On level 1, the order of the four symbol values is 1, 3, 2, 0. On higher levels, we find the same order if the total number of 1's and 3's taken together is even and the reversed order if this number is odd. This rule also applies to the order of 1 and 0 if the symbols 2 and 3 are missing at some node. The grammatical rules are read off as:

(i) on a symbol string ending on 0 or on +1, it is allowed to append 0 or 1 or 2 or 3;

(ii) on a symbol string ending on 2 or on 3, it is only allowed to append +;

(iii) on a symbol string ending on 11, 01 or +, it is allowed to append 0 or 1.

The non-trivial factor in the characteristic polynomial of the corresponding transfer matrix is

$$P(\lambda) = \lambda^4 - 2\lambda^3 - 4\lambda + 4. \tag{6}$$

Its largest root is $\lambda_{max} = 2.4019\ldots$. This value coincides with the average branching ratio of the intervals in the modified delay function.

Note that the fixed points belonging to the symbol values 2 and 3 have already been lost for the parameter value shown in figures 11(b) and 9. Correspondingly, infinite strings of 2's and 3's only are not allowed. Now the orbit Γ is unstable and it is accessible to scattering trajectories, therefore infinite strings of 1's are now allowed in contrast to the rules for $E \in I_{1/2}$ given in section 4. In analogy to the case considered in sections 3 and 4,

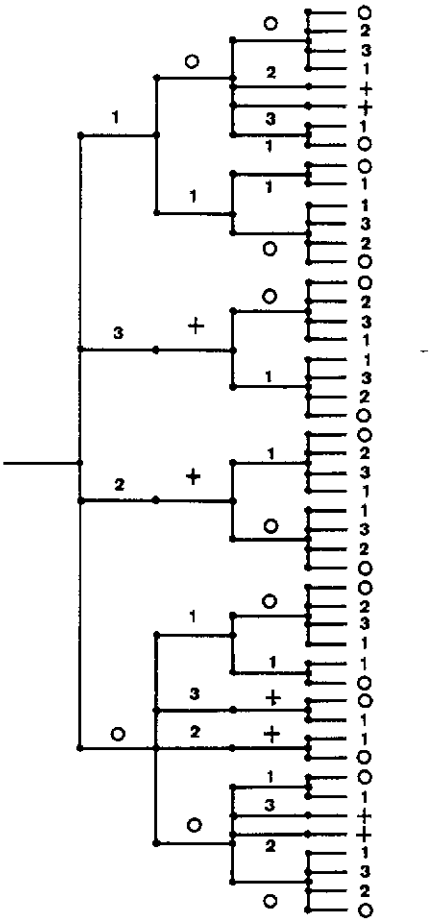

Figure 12. Branching tree corresponding to figures 9 and 11(*b*). Each entry is labelled by the last digit of its symbolic code.

it is again possible to avoid the introduction of the symbol + at the price of cutting some entries of the branching tree into two pieces.

For other parameter intervals in which homoclinic bifurcations are avoided (at least in low levels of the hierarchy), we can construct branching trees and symbolic codes along the same basic pattern (at least approximately).

6. Discussion

We have applied some ideas on the symbolic ordering of scattering functions on the motion of a charged particle in the field of a magnetic dipole. For some parameter regions, we have presented a simple symbolic dynamics. The intervals in which such a construction is possible are the ones in which homoclinic bifurcations are avoided. In our construction of the hierarchical order, two points are remarkable in our opinion.

(i) We look for the levels of hierarchy in an appropriate Poincaré map. The level of hierarchy of any trajectory is the number of its points which are located inside the fundamental area A of the horseshoe construction. This order does not coincide, in general, with the ordering provided by the true time delay function. Our modified delay function via the Poincaré map has the disadvantage that it cannot be constructed by the sole knowledge

of asymptotic scattering data, in contrast to the true time delay function. On the other hand, the true time delay function has the big disadvantage that it does not reveal the simple hierarchical order contained in the horseshoe construction. Note that, in general, the return times in a Poincaré section can be strongly different for different points.

(ii) It is useful (although not necessary) to have a number of symbol values which are larger than the number of fixed points of the Poincaré map in order to use the invariant manifolds of x_0 only for the partition. Thus, we can assign exactly one symbol sequence of length n to each interval J_k^n. It is not necessary to introduce further unnatural divisions which are necessary if we refuse to introduce additional symbols. The new symbol values (in the cases presented above, it is the +) correspond to blocks in which gaps of the corresponding complete horseshoe have disappeared and thereby distinct blocks of the complete case have been fused into a single block. For other parameter values or for other systems, this principle may require several different new symbol values for various different combinations of basic symbols.

In complete analogy to the extensive discussion given in [7], our symbolic description will break down for high levels in the hierarchy if the phase space of the system contains KAM lines, cantori or other subsets of marginal stability. In their vicinity, a symbolic dynamics with finite rules is no longer able to separate all the different trajectories. This breakdown should occur at such levels of the hierarchy where, in previous treatments of systems with incomplete horseshoes, a crossover from hyperbolic to non-hyperbolic behaviour has been observed [28–32].

Knowledge of a symbolic dynamics can also be useful in organizing the summation in a semiclassical treatment either by summing the amplitude directly [33] or by using periodic-orbit methods [34], where the symbolic dynamics tells us which periodic orbits are relevant for the scattering behaviour.

Acknowledgment

This work has been supported financially by the Deutsche Forschungsgemeinschaft.

References

[1] Cvitanovic P, Gunaratne G and Procaccia I 1988 *Phys. Rev.* A **38** 1503
[2] Auerbach D and Procaccia I 1990 *Phys. Rev.* A **41** 6602
[3] Jung C and Richter P 1990 *J. Phys. A: Math. Gen.* **23** 2847
[4] Troll G 1991 *Physica* **50D** 276
[5] Troll G 1992 *Nonlinearity* **5** 1151
[6] Vollmer J and Breymann W 1993 *Helv. Phys. Acta* **66** 91
[7] Rückerl B and Jung C 1994 *J. Phys. A: Math. Gen.* **27** 55
[8] Störmer C 1907 *Arch. Sci. Phys. Nat.* **24** 113
[9] Braun M 1970 *J. Diff. Eqns* **8** 294
[10] Contopoulos G and Vlahos L 1975 *J. Math. Phys.* **16** 1469
[11] Dragt A J and Finn J M 1976 *J. Geophys. Res.* **81** 2327
[12] Jung C and Scholz H J 1988 *J. Phys. A: Math. Gen.* **21** 2301
[13] Almeida M A, Moreira I C and Yoshida H 1992 *J. Phys. A: Math. Gen.* **25** L227
[14] Eckhardt B 1988 *Physica* **33D** 89
[15] Smilansky U 1992 *Proc. 1989 Les Houches Summer School* ed M J Giannoni, A Voros and J Zinn-Justin (Amsterdam: North-Holland) pp 371–441
[16] Tel T 1990 *Directions in Chaos* vol 3, ed Bai-lin Hao (Singapore: World Scientific) pp 149–221
[17] Tel T 1989 *J. Phys. A: Math. Gen.* **22** L691

[18] Kovacs Z and Tel T 1990 *Phys. Rev. Lett.* **64** 1617
[19] Brumer P and Shapiro M 1988 *Adv. Chem. Phys.* **70** 365
[20] Petit J M and Henon M 1986 *Icarus* **66** 536
[21] Eckhardt B and Aref H 1988 *Phil. Trans. R. Soc.* A **326** 655
[22] Campbell D K, Peyrard M and Sodano P 1986 *Physica* **19D** 165
[23] Jung C and Ziemniak E 1992 *J. Phys. A: Math. Gen.* **25** 3929
[24] 1993 *Chaos* **3** no 4
[25] Smale S 1967 *Bull. Am. Math. Soc.* **73** 747
[26] Davis M J, MacKay R S and Sannami A 1991 *Physica* **52D** 171
[27] Breymann W and Jung C 1994 *Europhys. Lett.* **25** 509
[28] Karney C F 1983 *Physica* **8D** 360
[29] Meiss J D and Ott E 1985 *Phys. Rev. Lett.* **55** 2741
[30] Ding M, Bountis T and Ott E 1990 *Phys. Lett.* **151A** 395
[31] Lau Y T, Finn J M and Ott E 1991 *Phys. Rev. Lett.* **66** 978
[32] Breymann W, Kovacs Z and Tel T 1993 Chaotic scattering in external fields *Preprint*
[33] Jung C and Pott S 1990 *J. Phys. A: Math. Gen.* **23** 3729
[34] Cvitanovic P and Eckhardt B 1989 *Phys. Rev. Lett.* **63** 823